

# Electrical Breakdown Currents on Large Spacecraft in Low Earth Orbit

Jason A. Vaughn\* and Melvin R. Carruth Jr.†  
NASA Marshall Space Flight Center, Huntsville, Alabama 35812  
and  
Ira Katz,‡ Myron J. Mandell,§ and Gary A. Jongeward¶  
Maxwell Laboratories, Inc., La Jolla, California 92038

An experimental and theoretical investigation of an expanding plasma generated by an arc produced by biasing a conductor underneath a thin layer of anodized aluminum 160-V negative of a laboratory plasma that can produce large peak arc currents by discharging large surface areas is presented. A simple theory shows that the time scales and observed current magnitudes are consistent with the expansion of a discharge-generated plasma. The implication for large spacecraft in low Earth orbit, such as Space Station Freedom (SSF) which can store large amounts of charge, is that arcs with the same amount of energy similar to those observed in the laboratory may occur. The energy in these arcs degrade the surface of the anodized aluminum thermal control coatings by producing large pits in the surface. These pits tend to increase the temperature of the spacecraft, and the material from the pits can become an additional source of contamination. The rise time and intensity of these arcs could produce significant EMI. To prevent the occurrence of these undesirable effects, SSF will utilize a plasma contactor that will control the structure to ambient plasma potentials.

## Nomenclature

$C$  = capacitance, F  
 $E$  = capacitive energy, J  
 $J_{th}^e$  = thermal electron current, A  
 $J_{th}^i$  = thermal ion current, A  
 $k$  = Boltzman's constant,  $1.38 \times 10^{-23}$  J/K  
 $n_e$  = electron density,  $\text{cm}^{-3}$   
 $n_i$  = ion density,  $\text{cm}^{-3}$   
 $n_0$  = electron density when  $\phi = 0$ ,  $\text{cm}^{-3}$   
 $q$  = electronic charge,  $1.6 \times 10^{-19}$   
 $T_e$  = electron temperature, eV  
 $t$  = time, s  
 $V_f$  = plasma front velocity, m/s  
 $x$  = plate separation distance, cm  
 $\phi$  = potential, V  
 $\phi_B$  = anodized aluminum bias potential, V  
 $\phi_s$  = plate surface potential, V  
 $\omega_{pi}$  = ion plasma frequency,  $\text{s}^{-1}$

## Introduction

SPACECRAFT operating in low Earth orbit (LEO) use solar arrays to convert photon energy from the sun into electrical energy for spacecraft power. Solar arrays of spacecraft requiring minimal amounts of power usually have operating voltages near 30 V. The only past experience with high

voltage arrays in space, which were near 90 V, was with Skylab.<sup>1</sup> As spacecraft become larger and more complex, they require more power to operate, as in the case of Space Station Freedom (SSF). To provide the required power for SSF, the voltage generated by the solar arrays had to be increased to avoid the need for developing large electrical distribution systems capable of handling large currents. The 160-V arrays of SSF have placed it in a regime where the physical interactions between the solar arrays<sup>2-5</sup> and the LEO plasma can be significant.

An illuminated solar array in the LEO ionosphere will reach an electrical equilibrium point with the ambient plasma, such that it collects net zero current from the plasma (i.e., floating potential). Because thermal electrons are lighter and, therefore, more mobile than thermal ions, they are collected easily by the array. The potential of the array must distribute itself relative to the local plasma to collect net zero current, which means a large portion of the solar array will be negative of the ambient plasma to collect the required amount of ions. Laboratory and flight data have shown this to be the case.<sup>6-9</sup> Because the common practice is to ground or reference the spacecraft to the negative side of the solar array, the spacecraft structure will be floating negative relative to the local plasma. Indeed, the structure will collect ions, but unless there is a very significant collection area, the floating potential distribution of the total system will not be significantly reduced. For these higher powered spacecraft, this places the spacecraft surface highly negative of the ambient plasma. In the case of SSF, the structure will charge to approximately 120–140 V negative of plasma potential unless active measures are taken to control it.<sup>10</sup> Because of the severe floating potential that SSF was predicted to experience, a plasma contactor is being designed to actively control the floating potential near that of the plasma. This paper will continue to use SSF design and material examples since SSF issues drove this study.

To keep the temperature of the spacecraft surface within design limits, thermal control coatings are applied to provide the surface emissivity and absorptivity necessary to control the temperature. Thermal control coatings that are good thermal isolators also tend to be good electrical insulators, producing undesired charging effects in LEO. In the past, paints that absorb and radiate the correct amount of heat have been used. For SSF, the selected coating is anodized aluminum with an

Presented as Paper 92-0822 at the AIAA 30th Aerospace Sciences Meeting, Reno, NV, Jan. 6–9, 1992; received June 26, 1992; revision received Nov. 9, 1992; accepted for publication Jan. 22, 1993. Copyright © 1993 by the American Institute of Aeronautics and Astronautics, Inc. No copyright is asserted in the United States under Title 17, U.S. Code. The U.S. Government has a royalty-free license to exercise all rights under the copyright claimed herein for Governmental purposes. All other rights are reserved by the copyright owner.

\*Materials Engineer, Physical Sciences Branch.

†Chief, Physical Sciences Branch. Member AIAA.

‡Senior Vice President, Manager, Space Systems Sector, S-Cubed Division. Member AIAA.

§Senior Scientist, Space Physics Group, S-Cubed Division. Member AIAA.

¶Vice President, Manager, Space Physics Group, S-Cubed Division. Member AIAA.

anodic thickness of 1.3–5.1  $\mu\text{m}$ . The thickness of these anodized coatings has been tailored to provide the correct thermal control properties necessary to control external surface temperatures. These thin coatings, however, do not have the dielectric strength to withstand the 120–140 V potential relative to the ambient plasma applied across the anodized layer due to the grounding of the negative side of the solar array to the structure.

A spacecraft immersed in the LEO plasma with a thin dielectric coating, such as anodized aluminum, will build up a large capacitive charge. Electrons that are collected by the solar array are stored near the interface of the bulk material and the anodic coating, and the net positive charge from the ambient plasma will be collected on the space side of the anodic coating. If the dielectric strength of the coating is not sufficient to withstand the applied voltage stress, dielectric breakdown will occur. Dielectric breakdown has been observed in the Marshall Space Flight Center tests at applied voltages as low as  $-80\text{ V}$  for some anodized aluminum surfaces.<sup>10</sup>

Laboratory measurements of the arc's intensity indicate it is a function of the stored energy in the thin dielectric layer of the SSF structure. Arc currents on the order of 1000 A were detected when enough capacitance to simulate a single SSF module was added to the test circuit in the laboratory.<sup>10</sup> The large amount of energy being released caused the anodic coating to pit and discolor, degrading the thermal control properties.<sup>11</sup> This leads to higher temperatures on the spacecraft surface. The debris being released by the pitting of the surface also becomes an additional source of contamination for sensitive optics.<sup>12</sup> The large currents observed during the laboratory tests could not have been supported by the dilute laboratory plasma. In this paper a mechanism for producing these large currents is presented. This mechanism involves the production and expansion of a dense arc plasma at the arc site. In the laboratory the large arc currents measured were produced by supplying large capacitance to the arc site. In space the only source of capacitance is the charge buildup produced by the dielectric anodized aluminum surface of the spacecraft. To understand the ability of the spacecraft in space to supply these large amounts of charge to the arc site producing large peak currents, tests were done to examine the ability of the arc to discharge surrounding anodized aluminum surfaces to provide the charge to drive these large arcs in space. A simple theoretical approach was taken to model the experimental data using previously developed models of plasma expansion into a vacuum and applying them to this case. The results of this model can then be applied to predict possible currents on SSF-sized structures in LEO.

### Experimental Test Apparatus

Ground tests were performed to simulate dielectric breakdown of thin anodized aluminum coatings in space in a 1.2-m-

### Two Plate Experiment Schematic

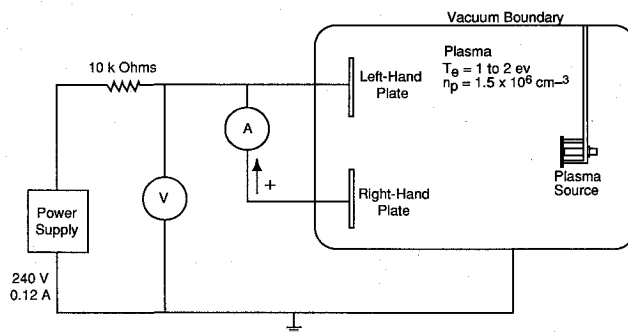


Fig. 2 Two-plate experiment test configuration.

diam  $\times$  1.8-m-long cylindrical vacuum chamber capable of a base pressure in the high  $10^{-8}$  Torr range. An argon plasma with density of  $10^6 \text{ cm}^{-3}$  and electron temperature of 1 eV to 2 eV was produced in the chamber using a hollow-cathode plasma source.<sup>13</sup> A hollow-cathode plasma source was chosen for these tests because of its ability to produce a fairly uniform, unperturbed plasma. Because a hollow-cathode plasma source requires a large gas flow to operate, the pressure during operation of the source was in the low  $10^{-4}$  Torr range. During testing, the plasma source was designed to float with respect to the ambient plasma in the tank, causing the ambient plasma floating potential to be close to zero volts with respect to ground.

The test articles used in these experiments were chromic-acid anodized aluminum plates with an anodic thickness layer ranging from 1.3 to 2.6  $\mu\text{m}$ . The type of anodized aluminum and range of oxide thicknesses were chosen because of the direct implication they have as the baselined material for the SSF meteoroid/debris shields. The back sides of the 7.6- $\times$  12.7-cm samples were coated with Kapton to insulate them from the plasma and restrict the discharges to the sample's front surface.

Figure 1 shows the test configuration used to measure the arc plasma expansion velocity. A single anodized aluminum plate was placed in the chamber and biased 160 V negative relative to ground by a power supply. The power supply was isolated from the sample by a 10-k $\Omega$  resistor so that only the energy stored in the plates anodization layer would discharge into the arc due to spontaneous dielectric breakdown. Because the plates themselves had a small capacitance, an 8- $\mu\text{F}$  capacitor was placed in the circuit to provide a charge reservoir. The 8- $\mu\text{F}$  capacitor was chosen because previous tests<sup>10</sup> which measured the peak arc currents as a function of capacitance showed the arc currents expected would be small, making measurements simpler. A 0.025-cm-diam and 12.7-cm-long cylindrical langmuir probe that could be moved axially from the anodized plate to the plasma source was placed in the chamber. The langmuir probe was grounded, and current to the probe was measured using an inductive current probe. One channel of an oscilloscope was connected to the inductive current probe and the other to the voltage bias on the plate. The oscilloscope was programmed to trigger on the change in the voltage bias on the plate, signaling the initiation of an arc. Current and voltage data were recorded for langmuir probe axial positions over a range of 50 cm in 5-cm increments. The data collected during these tests were used to calculate an arc plasma expansion velocity.

A second test configuration in which two anodized aluminum plates were placed in the chamber to examine the ability of the arc plasma to discharge remote anodized surfaces is shown in Fig. 2. The two plates were isolated from the vacuum chamber walls and each other within the chamber; however, the plates were connected by a single wire outside the vacuum chamber. The wire was made as short as possible to prevent

### Plasma Expansion Test Schematic

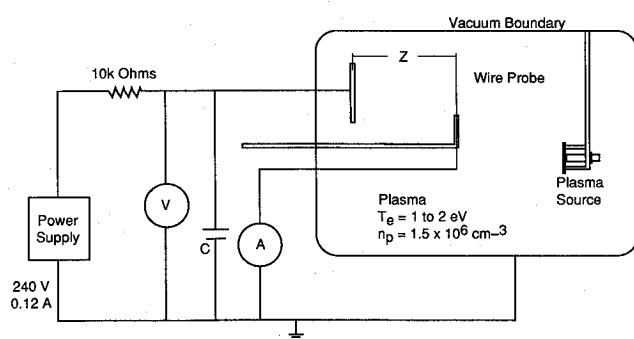


Fig. 1 Arc plasma expansion test schematic.

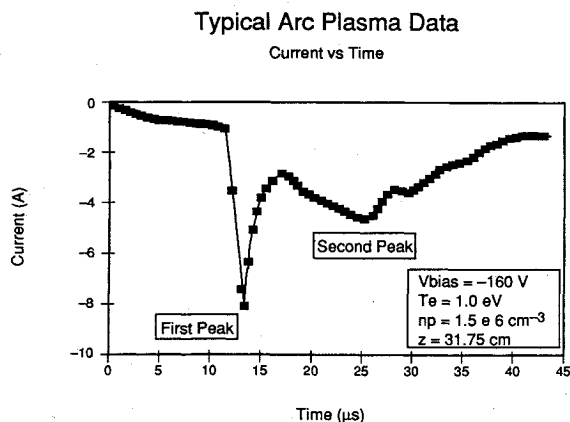


Fig. 3 Typical arc plasma expansion current vs time data.

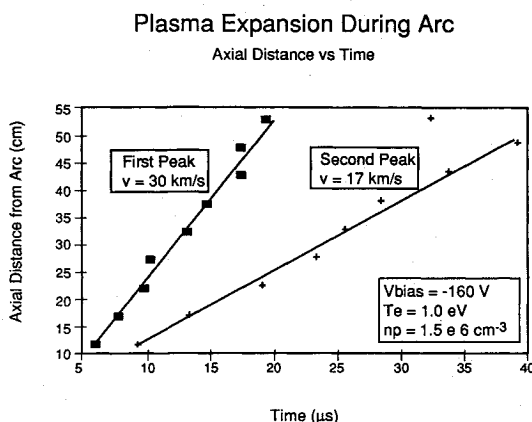


Fig. 4 Arc plasma peak current position vs time.

any inductive losses due to the wire itself. The two plates were spaced approximately 35 cm from the center of one plate to the center of the other. Figure 2 also shows the electrical schematic of the two-plate experiment. An inductive current probe was placed around the wire between the two plates to measure the current between the two plates during an arc. The oscilloscope that recorded the current data through the wire was triggered by the change in the voltage bias, signaling the initiation of the arc. The recorded current and voltage data were used to correlate the results of the first experiment by examining the lag time between the two. Only the stored capacitance ( $\approx 0.2 \mu\text{F}$ ) of the plates themselves could support arc currents in these experiments.

### Experimental Results

The initiation of an arc by dielectric breakdown causes electron current to flow from the structure to the arc site. To complete the circuit, the electrons must flow to the surface to neutralize the net positive charge. The flow of electrons begins with dielectric breakdown and the subsequent production of a dense arc plasma by vaporization and ionization of the bulk aluminum metal by the electrons, which are accelerated from the structure potential to plasma potential. The neutralization of the charge on the surface is facilitated by the expansion of the arc plasma.

Typical data collected while measuring the expansion rate of the arc plasma are shown in Fig. 3. The current trace presented in this figure was recorded with the langmuir probe approximately 32 cm from the anodized aluminum sample. All current traces recorded showed the two-peak structure observed in Fig. 3. The first peak shown in this figure is believed to be the wave front of the arc plasma passing the probe; but the origin of the second peak, which has a smaller intensity, is not

known at this time. The intensity of both fronts (i.e., 80 mA and 50 mA) is greater than the thermal electron current ( $0.1 \mu\text{A}$ ) that could be collected by the probe from the ambient plasma. This suggests the current being measured is a direct result of the much more dense arc plasma.

The time for the arc plasma wave front to reach the langmuir probe was plotted as a function of axial position and is shown in Fig. 4. This figure provides an indication of the velocity or the rate of expansion of the arc plasma into the ambient plasma. The electrostatic forces between both the ions and electrons suggests that both ions and electrons would be moving at nearly the same velocity. The velocities shown in Fig. 4 were computed by calculating the best linear fit to each set of data. The velocities calculated from the measured data are an order of magnitude higher than ion acoustic velocities of an aluminum plasma with an electron temperature on the order of 1 eV.

The intense arc plasma expands at a rate that seems to be controlled by the amount of energy supplied into it by the electrons stored just under the anodization layer. The arc plasma expands at a velocity sufficient to cover large surface areas of the anodized aluminum structure over a short period of time. The ability of the arc plasma to discharge the surface of the anodized aluminum structure was examined by placing two plates in a plasma. The plates were isolated from each other inside the chamber but connected outside as shown in Fig. 3. When one plate arced, the arc plasma would discharge the other plate, passing the stored charge of that plate between the two plates.

Typical current and voltage data recorded during the two-plate experiment are shown in Fig. 5. When these data were acquired, an arc occurred on the left-hand plate shown in Fig. 2. The time lag between the initiation of the arc, indicated by the increase in the voltage trace and the peak in the current trace, represents the time required for the plasma produced by the left-hand plate to discharge the right-hand plate. A simple calculation can be made of the time for the plasma to travel the distance from the right-hand plate to the left-hand plate. Assuming the dense arc plasma expands at the constant velocity indicated in Fig. 4, the time to reach the second plate could be computed using Eq. (1).

$$x = V_f t \quad (1)$$

The two plates are 35 cm apart from the center of one plate to the center of the other plate. A range of distances must be considered in this calculation because the exact location of the arc on a plate cannot be pinpointed. The range considered in this calculation was 31–39 cm, which is the distance from the center of one plate to both the near and far edges, respectively. The time for the plasma to reach the center of the second plate ranged from 10 to 13  $\mu\text{s}$ . Compared to the data shown in Fig.

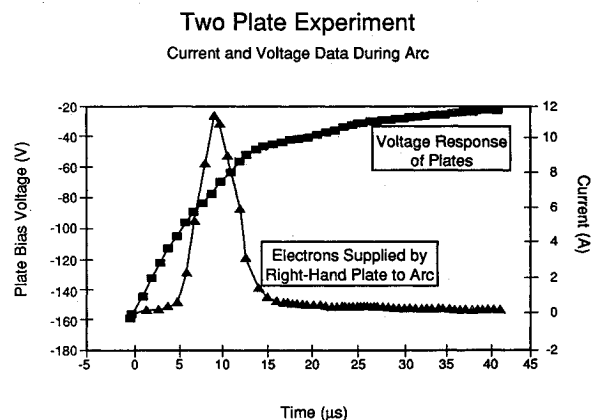


Fig. 5 Two-plate experiment typical current and voltage data.

5 this closely approximates the lag time between the start of the arc and the peak in the current trace. This suggests that the arc plasma can expand and discharge the neighboring anodized aluminum plate some 35 cm from the arc site.

The current being supplied from one plate to the other is shown in Fig. 6, and as would be expected the two current traces were mirror images of one another depending on which of the two plates arced. The current trace shown in the square data points was recorded when an arc occurred on the left-hand plate, the arc plasma expanded and discharged the right-hand plate. The right-hand plate then supplied the free electrons stored in the anodization layer to the arc site. The current trace shown in the triangular data was recorded when an arc occurred on the right-hand plate. The magnitude of the electron current being transferred between the two plates suggests that a large percentage of the plate is being discharged. The capacitance of the plates was calculated from the experimental data by numerically integrating the current data shown in Figs. 5 and 6 and dividing by the voltage drop. This capacitance agreed well with the theoretical capacitance calculated for one plate, assuming flat plate capacitance theory.

### Modeling

The experimental data suggest large arc currents can be generated by the expanding arc plasma based on the ability of the expanding plasma to discharge remote anodized surface areas. By discharging the ambient anodized aluminum surface, the charge stored in the aluminum conductor is available to drive the arc, producing large peak currents. This theory is strictly dependent on the physics of the expanding plasma. Other factors, such as geometry, may limit the magnitude of the peak current observed. To be able to predict the magnitude of possible arc currents on a large spacecraft in LEO based on the experimental data, a model was developed based on previous work with plasmas expanding into a vacuum.<sup>14-16</sup> Because the arc plasma is much more dense than the surrounding ambient plasma, the use of these models is a good approximation.

When exposed to the plasma environment, the negatively biased plates attract ions until the potential on the outer

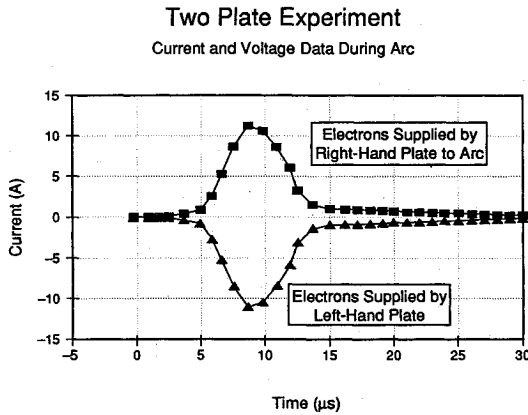


Fig. 6 Two-plate experiment current vs time.

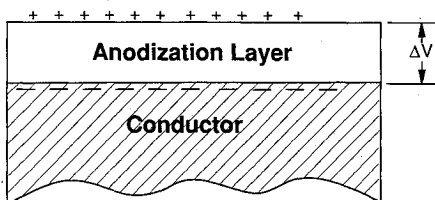


Fig. 7 Collection of charge across anodization layer.

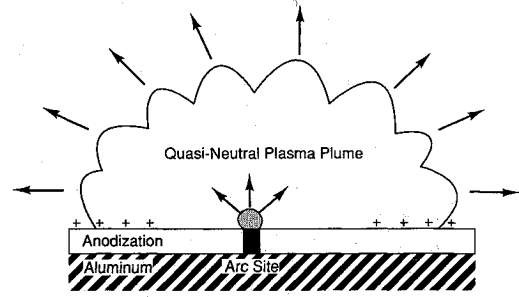


Fig. 8 Arc plasma expansion process.

surface of the anodization is such that the plate ion flux is balanced by the flux of plasma electrons (Fig. 7). Current balance occurs when the ion charge layer produces a voltage drop across the anodization layers sufficient to bring the surface to a few  $kT_e$  of the plasma potential.

At the surface, the electron ion current balance is achieved by repelling a fraction of the electrons.

$$J_{th}^i = J_{th}^e \exp(-q\phi_s/kT_e) \quad (2)$$

Prior to the breakdown, energy has been stored across the charged anodization layer in the electric field.

$$E = \frac{1}{2} C \Delta \phi_B^2 \quad (3)$$

When the plates are isolated from the chamber wall, this energy drives the discharge. For a spacecraft in orbit, the energy available is significant due to the large area of anodized aluminum exposed to the ionosphere. During the discharge, stored electron energy is released by currents flowing in a dense, self-generated plasma discharging the surface capacitance.<sup>14</sup> This process is depicted in Fig. 8. Material is vaporized and partially ionized at the arc site, as well as electron bombardment releasing and partially ionizing adsorbed gases as the discharge progresses along the surface. The implication is that all charged anodized surfaces near a breakdown site will be discharged during the breakdown, producing very large surface currents.

A plasma expands rapidly into a vacuum when electrostatic forces prevent the faster moving electrons from escaping the heavier, slower ions.<sup>15</sup> The quasineutrality conditions which prevent electron-ion charge separation that drive the expansion of the plasma into a vacuum are given in Eq. (4).

$$n_e = n_0 \exp(q\phi/kT_e) \quad (4)$$

where  $n_e \approx n_i$ .

Equation (4) is valid in the bulk of the expanding plasma but breaks down at the sharp front where the density of ions goes to zero. At the front and beyond, it is necessary to solve Poisson's equation to determine the cloud expansion.

A previous study<sup>16</sup> investigated the short and long time behavior of the  $\nabla\phi$  induced acceleration of a planar front. The analytic form plotted in Fig. 9 was found to connect these two limiting regimes and compared well with laboratory data of plasma front expansion. Note that the velocity of the expanding cloud becomes several times the sound speed for long times compared with the plasma period of the expanding arc cloud. In this regime, the expansion velocity is a slowly rising (logarithmic) function of time and is nearly constant with magnitude 5-10 times the sound velocity.

The preceding analysis is only qualitatively correct for the spherical plasma cloud of an arc discharge. For this case, we resort to numerical simulations. A standard water bag approach was taken and consists of the following steps: 1) A stationary plasma cloud was placed in a spherical grid with equal mass shells. 2) Poisson's equation was solved for the given ion density and barometric electrons described in Eq.

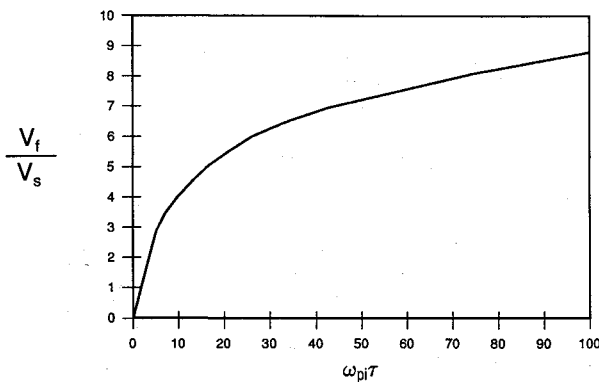


Fig. 9 Plasma wave front velocity, sound speed ratio vs ion plasma frequency.

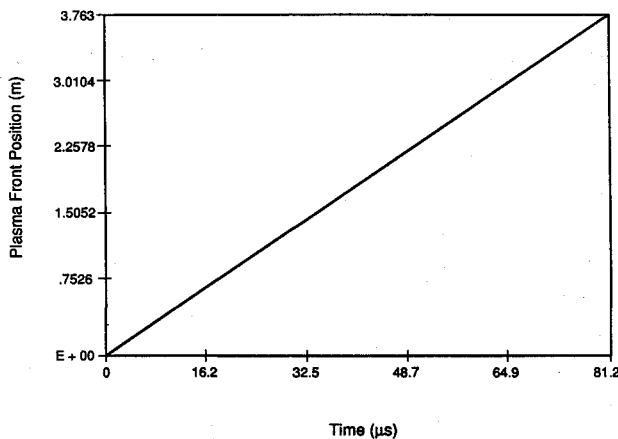


Fig. 10 Numerical simulation of expanding spherical plasma cloud.

(4). 3) The plasma ions are time stepped under the influence of  $\nabla \phi$ . 4) The ion density is recomputed. 5) Steps 2-4 are iterated to the desired time.

To simulate the expansion of an arc, a plasma sphere with  $10^{13} \text{ cm}^{-3}$  plasma density and a 1-mm radius, which is representative of a dense plasma, was placed at the origin and allowed to expand following steps 1-5. For this case, the expanding front position as a function of time is shown in Fig. 10. Here,  $\omega_{pi} = 10^9/\text{s}$ , so the plasma accelerates to the regime where the velocity increases only logarithmically in a few tenths of a microsecond. After this initial period, the plasma continues to expand with an approximately constant velocity of 46 km/s.

The experimental data shown in Figs. 4-6 verifies both the expanding plasma cloud concept, and that the cloud discharges the charge stored in the anodization layer. As shown in Fig. 4, the expansion velocity as measured by placing probes at various distances from the arc show the velocity of the front to be approximately 30 km/s in agreement with the earlier analysis. Additionally, this expansion process is seen in the time lag between the onset of current from the second plate and the arc initiation time on the first plate.

The magnitude of the discharge current is also consistent with this discharge mechanism. The expanding plasma moves over the second plate with a velocity  $V_f$  discharging the surface. As the surface discharges, a current is produced proportional to this velocity, given by Eq. (5).

$$I = V_f(C/l)\Delta\phi \quad (5)$$

Where  $(C/l)$  is the capacitance per unit length of the anodized plate in the direction of the front velocity. This equation assumes flat plate capacitance theory and that the expanding

plasma instantaneously discharges the width of a single sample as it expands across the plate. Using the measured value for the expansion velocity,  $V_f$ , 30 km/s and the plate capacitance per unit length of  $1.8 \times 10^{-6} \text{ F/M}$  assuming a constant width of 0.127 m, an anodic coating thickness of  $1.3 \mu\text{m}$ , and a dielectric constant of 2 gives a discharge current of 8 A in agreement with the 12-A peak current measured.

Predicting the arc current magnitude for other, more complex spacecraft geometries such as SSF is difficult because it is dependent on the ability of the plasma to expand and discharge remote surface areas. For large planar structures, if one assumes hemispherical expansion of the plasma, the current rises as the radius of the expanding plasma cloud increases and discharges the anodization layer, producing very large currents for large planar areas. It is expected that other mechanisms will limit the range of the interaction and hence the maximum currents expected. In contrast, for small cylindrical structures, not enough energy can be dumped to the arc to support the expanding plasma once the cloud radius is larger than the radius of the cylinder.

### Summary

The size and power requirements of SSF raised the need to consider new environmental interactions between the LEO plasma, the SSF structure, and the power system. For high voltage systems and present design practice, which grounds or references the structure to the negative side of the solar array, dielectric breakdown will occur on spacecraft whose potential relative to the plasma is greater than the dielectric strength of the insulative coatings. During the breakdown of the dielectric coating on the anodized surface covering the structure, there is sufficient energy to vaporize and ionize the aluminum structure at the arc site, producing a dense arc plasma. The arc plasma expands hemispherically from the arc site at a rate many times the ion acoustic velocity. As the arc plasma expands along the surface, it neutralizes the net positive charge that has collected along the structure by providing a low-impedance current path through the arc site to the underlying conductor. The amount of charge neutralized by the arc plasma increases the intensity of the arc.

A theoretical model is presented that predicts the arc plasma cloud expansion velocity and discharge currents in rough quantitative agreement with the laboratory data. A preliminary numerical simulation of a fixed amount of expanding plasma agrees qualitatively with the analytical treatment and the experimentally measured expansion rates. Work is in progress to produce a three-dimensional simulation of the arc plasma cloud expansion, including self-consistent discharge plasma generation rate, the background plasma pileup, and surface discharging.

### References

- <sup>1</sup>Bechtel, R. T., private communication, Marshall Space Flight Center-Electrical Div., Marshall Space Flight Center, AL, Oct. 1991.
- <sup>2</sup>Kennerud, K. L., "High Voltage Array Experiments," NASA CR-121280, March 1974.
- <sup>3</sup>Stevens, N. J., Berkopce, F. D., Purvis, C. K., Grier, N., and Staskus, J., "Investigation of High Voltage Spacecraft System Interactions With Plasma Environments," AIAA Paper 78-672, April 1978.
- <sup>4</sup>McCoy, J. E., and Konradi, A., "Sheath Effects Observed on a 100 Meter High Voltage Panel in Simulated Low Earth Orbit," *Spacecraft Charging Technology-1978*, NASA CP-2071, Oct.-Nov. 1978, pp. 315-340.
- <sup>5</sup>Grier, N. T., and Stevens, N. J., "Plasma Interaction Experiment (PIX) Flight Results," *Spacecraft Charging Technology-1978*, NASA CP-2071, Oct.-Nov. 1978, pp. 295-314.
- <sup>6</sup>Kerslake, W., and Domitz, S., "Neutralization Tests on the SERT II Spacecraft," AIAA Paper 79-2064, Oct.-Nov. 1979.
- <sup>7</sup>Grier, N. T., "Plasma Interaction Experiment II (PIX-2): Laboratory and Flight Results," *Spacecraft Environmental Technology-1983*, NASA CP-2359, Oct. 1983, pp. 333-348.
- <sup>8</sup>Grier, N. T., "Experimental Results on Plasma Interactions with Large Surfaces at High Voltages," NASA TM-81423, Jan. 1980.

<sup>9</sup>Jones, S., Staskus, J., and Byers, D., "Preliminary Results of SERT II Spacecraft Potential Measurements Using Hot Wire Emissive Probes," AIAA Paper 70-1127, Aug.-Sept. 1970.

<sup>10</sup>Carruth, M. R., Jr., Vaughn, J. A., and Gray, P. A., "Experimental Studies on Spacecraft Arcing," AIAA Paper 92-0820, Jan. 1992.

<sup>11</sup>Carruth, M. R., Jr., Vaughn, J. A., Holt, J. M., Werp, R., and Sudduth, R. D., "Plasma Effects on the Passive Thermal Control Coatings of Space Station Freedom," AIAA Paper 92-1685, March 1992.

<sup>12</sup>Carruth, M. R., Jr., Norwood, J. K., and Vaughn, J. A., "Arc Contamination Source Studies," *Proceeding of SSF Electrical Grounding Tiger Team Meeting*, Cleveland, OH, Sept. 1991, pp. 65-75.

<sup>13</sup>Siegfried, D. F., "A Phenomenological Model for Orificed Hollow Cathodes," NASA CR-168026, Dec. 1982.

<sup>14</sup>Pillai, S., and Hackam, R., "Surface Flashover Of Solid Dielectric In Vacuum," *Journal of Applied Physics*, Vol. 53, No. 4, 1982, pp. 2983-2990.

<sup>15</sup>Crow, J. E., Auer, P. J., and Allen, J. E., "The Expansion of a Plasma into Vacuum," *Journal of Plasma Physics*, Vol. 14, Feb. 1975, pp. 65-76.

<sup>16</sup>Katz, I., Parks, D. E., and Wright, K. H., Jr., "A Model of the Plasma Wake Generated by a Large Object," *IEEE Transactions on Nuclear Science*, Vol. NS-32, Dec. 1985, p. 4092.

Alfred L. Vampola  
Associate Editor